

# Semiparametric Discovery and Estimation of Interaction in Mixed Exposures using Stochastic Interventions

David B. McCoy \*

Division of Biostatistics, University of California, Berkeley  
and

Alan Hubbard

Division of Biostatistics, University of California, Berkeley  
and

Mark van der Laan

Division of Biostatistics, University of California, Berkeley  
and

Alejandro Schuler

Division of Biostatistics, University of California, Berkeley

March 1, 2024

## Abstract

This study introduces a nonparametric definition of interaction and provides an approach to both interaction discovery and efficient estimation of this parameter. Using stochastic shift interventions and ensemble machine learning, our approach identifies and quantifies interaction effects through a model-independent target parameter, estimated via targeted maximum likelihood and cross-validation. This method contrasts the expected outcomes of joint interventions with those of individual interventions. Validation through simulation and application to the National Institute of Environmental Health Sciences Mixtures Workshop data demonstrate the efficacy of our method in detecting true interaction directions and its consistency in identifying significant impacts of furan exposure on leukocyte telomere length. Our method, called SuperNOVA, advances the ability to analyze multiexposure interactions within high-dimensional data, offering significant methodological improvements to understand complex exposure dynamics in health research. We provide peer-reviewed open-source software that employs or proposed methodology in the **SuperNOVA** R package.

*Keywords:* Targeted Maximum Likelihood Estimation, Mixtures, Interactions, Decision Trees, Ensemble Learning

---

\*The authors gratefully acknowledge funding for Core E of the NIEHS Superfund Center at Berkeley funded by NIH grant P42ES004705

# 1 Introduction

In environmental health research, understanding the impact of simultaneous multiple exposures on health outcomes is crucial yet challenging. Traditional epidemiological studies frequently rely on generalized linear models (GLM) to assess main effects, often neglecting complex interactions within exposure mixtures, potentially oversimplifying the intricate dynamics at play [García-Villarino et al. [2022]]. While methods such as Principal Component Analysis (PCA) and penalized regressions, such as LASSO and Ridge, address issues of high dimensionality and multicollinearity, they fall short in interpretability, especially in regulatory and policy contexts where specific guidance on exposure reduction is needed [Roberts and Martin [2006], ?], [McEligot et al. [2020]]. The limitations of existing approaches, including quantile sum g-computation and linear models without interaction terms, risk simplifying the nuanced effects of interactions [Keil et al. [2019]]. Bayesian Kernel Machine Regression (BKMR) offers a more nuanced framework employing Bayesian hierarchical models and kernel machine learning to evaluate high-dimensional exposure effects, providing uncertainty quantification through posterior distributions [Bobb et al. [2014]]. Despite BKMR's advantages, practical challenges emerge, particularly with defining interactions in high-dimensional settings (which two or three-way interactions to examine), which lead to combinatorial complexity and prioritization challenges for researchers. This backdrop underscores the necessity for our proposed method, which aims to accurately identify and estimate interactions in the context of environmental health research, thereby addressing the limitations of current methodologies.

Given that interactions in a mixed-exposure setting are not known a priori, data-driven approaches for interaction identification are critical. The functional ANOVA (fANOVA) technique, for example, developed to detect interactions in flexible models, such as tree-based

or additive models, is one of such approaches. Lengerich et al. [2020]. However, fANOVA, like traditional ANOVA, primarily quantifies interaction effects in terms of the variance explained, which may not directly translate into actionable insights for epidemiologists or policy makers. Similarly, methods such as Narisetty et al. [2019] use a forward selection of expanded basis functions to find interactions. In both cases, although modeling informs what interaction improves model fit, there is no measure of causal association, which is more pertinent to inform policy decisions. Important insights have been provided on how to define interactions in a causal inference framework VanderWeele [2009], VanderWeele and Knol [2014], VanderWeele and Robins [2007], Rothman et al. [1980]. Much of this work has done so in the context of binary explanatory variables of interest. However, the wide range of exposures that characterize environmental investigations often render standard binary causal models inadequate. This accentuates the need for a versatile, semiparametric interaction definition that can accommodate a spectrum of data types, a current gap in methodologies.

Our proposed approach, termed **SuperNOVA**, synthesizes two critical phases of analysis, discovery and estimation, using the same data. Initially, we used an ANOVA-style decomposition to suggest interacting exposures in a semiparametric model via a sieve approach. Subsequently, we estimate the counterfactual effect of changing all of these exposures by a small amount versus the combined effects of changing them individually. The interaction discovery component of **SuperNOVA** is similar to the fANOVA approach for the discernment of interactions. However, our approach finds the best finite sample approximation in a model using ensemble learning of semiparametric maximum likelihood estimation regressions van der Laan Mark et al. [2007]. This leads to ANOVA over basis functions, which, when aggregated, offers holistic F-statistics sets for pivotal exposure sets used in the

best estimator. These exposure sets are then the target for our nonparametrically defined interaction parameter. Our target parameter evaluates the effect of feasible stochastic shift interventions on exposure distributions, as conceptualized in the literature Iván Díaz Muñoz and Mark van der Laan\* [2012]. Such interventions are highly relevant to public policy, as they often mirror the realistic impact of regulatory measures that aim to slightly reduce, rather than completely eliminate or uniformly standardize, exposures across a population. For example, we might consider the population-level effect of reducing everyone’s exposure to a persistent organic pollutant by a small, relative amount. Our parameter defines an interaction effect by comparing the expected outcome under a joint shift of exposures (like simultaneously reducing levels of a dioxin and PCB) against the summed expected outcomes of individual shifts. This approach offers a pragmatic and policy-relevant interpretation of interactions, grounded in causal assumptions, and is estimable from observational data using an asymptotically efficient targeted maximum likelihood estimator that facilitates the construction of confidence intervals and hypothesis testing.

The concurrent requirements of identifying (initially unknown) interacting variables and estimating their effects require a two-prong approach to prevent obvious overfitting. To address this, we split the full sample data: one segment identifies interactions and the other employs an efficient estimator for the data-adaptive target parameters. Our approach, termed **SuperNOVA** integrates estimates across different data splits with cross-validated targeted maximum likelihood (CV-TMLE) Hubbard et al. [2016], Zheng and van der Laan [2010]. **SuperNOVA** stands distinctively due to several key advantages. Firstly, it avoids bias of assuming linearity unlike techniques such as PCA or lasso. Although fANOVA and BKMR also embrace nonparametric approaches, **SuperNOVA** sets itself apart through its data-driven discovery of interactions. Contrary to approaches like fANOVA and BKMR, which estimate

the joint impact of all mixture variables, **SuperNOVA** offers a more practical solution to analyze high-dimensional mixtures in finite samples. It integrates a variable selection mechanism, focusing exclusively on those variables within the mixture that demonstrate statistically significant associations with the outcome of interest. This targeted approach in **SuperNOVA** not only improves efficiency, but also provides clearer insights into the key variables driving interactions in complex exposure scenarios. Additionally, its policy-relevant definition of interaction clearly marks an improvement over the aforementioned methods. The method’s scalability and speed of inference further bolster its appeal. By leveraging standard ML/TMLE tools, **SuperNOVA** avoids the pitfalls of bespoke optimization algorithms, such as those in fANOVA or time-consuming MCMC as seen in BKMR. In **SuperNOVA**, the use of data-adaptive estimators in both interaction identification and nuisance estimation is key. Moreover, the application of CV-TMLE ensures robust inference using the full dataset, thereby retaining power even when data is used for both parameter definition and estimation. However, in the case where the same interactions are not found in every fold of the CV procedure, the inferred null must be incorporated into a pooled result. We offer an approach to estimate pooled TMLE results for inconsistent interactions, which has higher power compared to simply reporting fold-specific results.

The structure of this paper is as follows. Section 2.1 provides a background on the semiparametric methodology that underpins stochastic interventions. Sections 2.2 and 2.3 delineate the interaction target parameter and the essential assumptions for our causal interpretations. Section 3. discusses the TMLE estimator. In Section 4. we discuss inference and elucidate our approach to determining variable sets. Section 5. presents simulation results, underscoring the asymptotic unbiasedness of our estimates. Section 6 demonstrates **SuperNOVA**’s applicability, juxtaposing it against existing techniques and

its relevance in real-world scenarios using synthetic data from the National Institute of Environmental Health Sciences (NIEHS). We provide real-world results when applying **SuperNOVA** to National Health and Nutrition Examination Survey, where we investigate the effects of 18 POPs on telomere length. In Section 7 we wrap up with a comprehensive discussion of strengths and weaknesses and provide our software.

## 2 Data and Parameter of Interest

### 2.1 Overview

At a high level, consider that an analyst has data on a mixture of 15 chemicals (e.g. 15 POPs). Our approach first splits the entire data into discovery and estimation samples. In the discovery sample, we employ versatile machine learning to identify interactions. For example, consider that we find an interaction between a POP-1 and POP-6. We then use the estimation portion of the data to estimate our interaction target parameter. Our interaction parameter is based on comparing a joint stochastic shift, that is, shifting both exposure simultaneously and observing the expected outcome and comparing this to the summed expected outcomes given individual shifts of each POP independently. We cycle through the data, for example, 10 times, and average estimates across the 10 folds using cross-validated targeted maximum likelihood estimation (CV-TMLE). Because our estimand depends on the data, if the full data were used to both discover and estimate, our statistical inference suffers from overfitting; thus, this data-splitting is necessary. With this example in mind, subsequent sections will delve deeper, elucidating each component of our parameter for enhanced clarity.

## 2.2 Notation and Framework

Building upon the concepts presented in Iván Díaz Muñoz and Mark van der Laan\* [2012] on stochastic interventions, we generalize this work to a target parameter that compares the expected outcome under a joint shift (here we focus on two exposures for brevity). As such, we first describe our target parameter for a stochastic shift of multiple exposures (which deviates little from estimating the impact of a stochastic shift of an individual variable) and then show how we can build our target parameter for interactions from this joint-shift target parameter. Consider an experiment in which a vector of exposure variables  $\mathbf{A}$ , a continuous or binary outcome  $Y$ , and a set of covariates  $W$  are measured for  $n$  randomly sampled subjects. Let  $O = (W, \mathbf{A}, Y)$  represent a random variable with distribution  $P_0$ , and  $O_1, \dots, O_n$  represent  $n$  i.i.d. observations of  $O$ . The true distribution  $P_0$  of  $O$  can be factorized as  $P_0(O) = P_0(Y|\mathbf{A}, W)P_0(\mathbf{A}|W)P_0(W)$ . We use  $p(\cdot)$  to denote the corresponding densities, e.g.  $p(Y|A, W)$ . The conditional joint density of exposures given covariates  $p(\mathbf{A}|W)$  we will refer to as  $g_0(\mathbf{A}|W)$  to distinguish it. Similarly we use  $\bar{Q}_0(\mathbf{A}, W) \equiv E_0(Y|\mathbf{A}, W)$ . We denote a “shifted” exposure density using the notation  $g_\delta(\mathbf{A}|W) = g_0(\mathbf{A} - \delta|W)$  and we denote the full “shifted” density over all variables as  $p_\delta(O) = p(Y|\mathbf{A}, W)g_\delta(\mathbf{A}|W)p(W)$ . In this section, while we theoretically describe the shifts  $\delta$  as fixed quantities (in particular, which variables are shifted at all and in what amounts), practical applications require them to be identified in a data-adaptive manner. We first describe the parameter that we will estimate treating exposure shifts as fixed, and then we describe how to identify what exposures to shift and by how much.

For example, consider  $A = (A_1, A_2)$  (e.g.,  $A_1$  = dioxin,  $A_2$  = furan, both POPs), here we are interested in the probability of the outcome given joint exposure. We are then interested in reducing this exposure profile by  $\delta = (\delta_1, \delta_2)$  which can be static (say some practical

unit or standard deviation) or this can be a function  $\delta(W)$ , that is, a change amount based on the history of the covariates. We use  $P$  to denote a generic probability distribution within a nonparametric statistical model  $\mathcal{M}$ . The symbol  $P_n$  represents the empirical distribution of the observed data, attributing a probability of  $\frac{1}{n}$  to each observation for the sample size  $n$ . The mapping of target parameters is defined as  $P \rightarrow \Psi(P)$ , with  $\Psi(P_0)$  as the true target parameter under  $P_0$ , and  $\hat{\Psi}(P_n)$  as an estimator mapping the empirical distribution  $P_n$  to its estimated value. The true value of the target parameter is  $\psi_0 = \Psi(P_0)$ , and its estimate based on  $P_n$  is represented as  $\psi_n$ . In causal inference, we often seek to contrast observed data with potential outcomes under different intervention scenarios (the full causal model). We begin by first clarifying the distinction between statistical and causal parameters for stochastic shift interventions for potentially multiple exposures, then we move on to build our parameter from this identification. We first define our causal parameter using counterfactuals Rubin [1974, 2005]. For each unit in our population, we have an infinite family of potential outcomes  $Y(\cdot)$  corresponding to every possible value of  $\mathbf{A}$ . This family,  $Y(\cdot)$ , is considered a stochastic process. In practice, for each unit, we observe only one of these potential outcomes, specifically  $Y(\mathbf{A})$ , the outcome corresponding to the observed treatment. However, we can define a true *causal* distribution  $P_0^*$  as a distribution over the variables  $Y(\cdot), \mathbf{A}, W$ . The condition  $Y = Y(\mathbf{A})$  defines a mapping  $\mathcal{O}$  from causal distributions  $P^*$  to observable distributions  $P$ . Our causal goal is to define potential outcomes via intervention on  $\mathbf{A}$  to a new value,  $\mathbf{A} - \delta$ . In this context, our causal parameter is defined with respect to the causal distribution  $P^*$ ,  $\Psi^*(P^*) = \mathbb{E}_{P^*}[Y(\mathbf{A} - \delta)]$ .

However, because  $P^*$  includes unobserved potential outcomes, we cannot estimate  $\Psi^*(P^*)$  directly. Instead, we rely on identification strategies that allow us to express the causal parameter  $\Psi^*(P^*)$  in terms of the observed data distribution, thereby allowing us



to make a practical estimation from the data we have. The assumptions needed for this are conditional ignorability:  $Y(a) \perp A|W$  for all  $a$  and positivity:  $0 < \frac{g_\delta(A|W)}{g(A|W)} < M$  with probability 1. With these assumptions, we can identify our causal parameter via the following statistical parameter  $\Psi(P) = E_{P_\delta}[Y] = \int_{\mathbf{A}} \int_W \bar{Q}(\mathbf{a}, w) g_\delta(\mathbf{a}|w) p(w) d\mathbf{a} dw$ . This captures the distribution of outcomes  $Y$  if we were to simply change the observed exposure  $\mathbf{A}$  by some amount  $\delta$ , while keeping all other factors unchanged. Throughout, let  $E_\delta[\cdot]$  abbreviate  $E_{P_\delta}[\cdot]$ . Note that despite being defined in terms of  $P_\delta$ ,  $\Psi(P)$  is indeed a function of  $P$  because  $P_\delta$  is defined in terms of  $P$ . Thus, upon invoking these assumptions,  $\Psi^*(P^*) = \Psi(\mathcal{O}(P^*)) = \Psi(P)$ . From now on, we focus on the target parameter  $\Psi$  (defined on the observable distribution) and our observable estimand  $\psi_0$  (the value  $\Psi$  takes at our true, unknown distribution  $P_0$ ). In practice, identifying causal effects requires thorough consideration of these assumptions. The conditional ignorability assumption, in particular, asserts that there are no unmeasured confounders influencing both the exposure and the outcome, which is a substantial claim, especially in observational data where mixed exposures are usually observed. The positivity assumption ensures that there is enough variability in our data to make meaningful causal inferences. When these assumptions are reasonable and satisfied, the statistical parameters derived from the observed data can be insightful proxies for the true causal parameters. Alternatively, the resulting quantities can be interpreted as pure statistical parameters of interest, a particular type of association of  $A$  with  $Y$  controlling for  $W$ , van der Laan [2006]. In this way, we can interpret “causal parameters” as a variable importance measure.

## 2.3 Interaction Target Parameter

Our target parameter above defines the causal parameter for an arbitrary joint shift of multiple exposures under the stochastic intervention framework. Realistically, given the

usual size and complexity of public health data, no more than two-way interactions can normally be reliably determined. As such, we focus on describing the interaction parameter for two exposures that builds off the joint stochastic shift parameter previously discussed; it is straightforward to generalize the above to more than two exposures. The symbol  $\delta$  in bold represents the shift of both exposures by two shifted amounts,  $E_{\delta_1}[Y]$  represents the change in  $A_1$  by  $\delta_1$  leaving  $A_2$  at the observed levels, and  $E_{\delta_2}[Y]$  represents a shift in  $A_2$  by  $\delta_2$  leaving  $A_1$  at the observed levels. As such, we define our bivariate interaction parameter  $E_{\delta}[Y] - (E_{\delta_1}[Y] + E_{\delta_2}[Y]) + E[Y]$ . Which is the expected outcome under the joint shift of  $\mathbf{A}$  compared to the expected additive outcome under each individual shift in  $\mathbf{A}$ . The interpretation of this parameter is similar to that of an interaction term in a linear model.

### 3 Estimation and Interpretation

#### 3.1 Efficient Influence Function

In expanding the scope of Diaz and van der Laan's work on TMLE for these shift intervention parameters Iván Díaz Muñoz and Mark van der Laan\* [2012] to consider exposures as vectors rather than scalar entities, we simply modify the notation to possible sets of exposures accordingly. The EIF for  $E_{\delta}[Y]$  is given by  $D_{\delta}(P_0)(o) = H_{\delta}(\mathbf{a}, w)(y - \overline{Q}(\mathbf{a}, w)) + \overline{Q}(\mathbf{a} - \boldsymbol{\delta}, w) - E_{\delta}[Y]$ . Where  $H_{\delta}$  is defined as  $H_{\delta}(\mathbf{a}, w) = \frac{g_0(\mathbf{a} - \boldsymbol{\delta} | w)}{g_0(\mathbf{a} | w)}$ . Note that vectors  $\mathbf{a}$  and  $\boldsymbol{\delta}$  emphasize the element-wise operations and comparisons. Extension to a vectorial representation allows us to use the original EIF for multiple exposures. The auxiliary covariate  $H_{\delta}(\mathbf{a}, w)$  serves as a ratio of conditional (possibly joint) densities  $p(\mathbf{a} | W)$ . Specifically,  $g_0(\mathbf{a} | w)$  denotes the conditional density under observed values, while  $g_0(\mathbf{a} - \boldsymbol{\delta} | w)$  is the density after a decrease of  $\boldsymbol{\delta}$  to  $\mathbf{a}$ . This ratio captures the density's change upon a  $\boldsymbol{\delta}$  shift. In

our approach, we use TMLE to remove the plug-in bias of our  $\bar{Q}$  estimators. Given the interaction parameter defined as  $\Psi(P) = E_{\delta}[Y] - (E_{\delta_1}[Y] + E_{\delta_2}[Y]) + E[Y]$ , the EIF for this interaction can be succinctly represented in terms of the EIFs for the individual components  $D(P) = D_{\delta}(P) - (D_{\delta_1}(P) + D_{\delta_2}(P))$ , where  $D_{\delta}(P)$  is the EIF of  $E_{\delta}[Y]$  and  $D_{\delta_1}(P)$  and  $D_{\delta_2}(P)$  are the EIFs of  $E_{\delta_1}[Y]$  and  $E_{\delta_2}[Y]$ , respectively.

### 3.2 TMLE

We chose to estimate our parameter using TMLE (rather than estimating equations, inverse propensity of treatment weights (IPTW) and augmented IPTW ) chiefly due to its favorable finite sample properties due to being a plug-in estimator. Briefly, to construct the TMLE estimator, we: 1. Use data-adaptive regression for the initial estimation of  $g_0(\mathbf{a}, W)$  and  $\bar{Q}_0(\mathbf{a}, W)$ , 2. Evaluate  $H(\mathbf{a}_i, w_i)$  for each observation, 3. Using the derived estimates, we implement a logistic regression to refine predictions under the shift  $\text{logit}\bar{Q}_{\epsilon,n}(\mathbf{a} - \delta, w) = \text{logit}\bar{Q}_n(\mathbf{a} - \delta, w) + \epsilon H_n(\mathbf{a} - \delta, w)$  then 4. From this model, once  $\epsilon$  is determined, we update the predicted counterfactuals, using these updated counterfactuals, we then compute the plugin. This is a standard TMLE procedure for stochastic interventions; we simply shift multiple exposures simultaneously in the initial estimation and update. We estimate a standard error by taking the empirical variance of the estimated EIF and use this construct Wald-type confidence intervals and p-values. We use TMLE to ascertain unbiased estimates for each part of our interaction target parameter. That is, in  $E_{\delta}[Y]$  we update our counterfactual outcome under a joint shift by the joint density ratio as  $H(\mathbf{a}, w)$ . Similarly,  $E_{\delta_1}[Y]$  and  $E_{\delta_2}[Y]$  are simply updated based on  $H(a, w)$  for univariate shifts. In general, we use TMLE to target each of the three parts of our parameter. Given that our interaction is a continuous function (linear combination) of these asymptotically efficient

estimates, we use the delta method for variance derivation.

### 3.3 Joint Density Estimation

In the context of extending the clever covariate to account for joint shifts, a challenge emerges when confronting the estimation of the joint density, especially in scenarios with high-dimensional  $W$ . Direct estimation of joint conditional densities using conventional techniques scales poorly to large data Chen et al. [2018]. To avoid the complications inherent in the direct estimate of joint density, we take an alternative approach. Instead of seeking an explicit joint density estimator, the methodology takes advantage of the combination of conditional and marginal densities. In the bivariate scenario involving exposures  $A1$  and  $A2$ , the joint density can be calculated more conveniently as  $g_0(\mathbf{A}|W) = g_0(A1|W) \times g_0(A2|A1, W)$ . Within this framework, two ensemble-based machine learning density estimators are deployed. The first is used to approximate the density of  $A1$  conditioned on  $W$ , while the second estimates the conditional density of  $A2$  given both  $A1$  and  $W$ . The product of these constructed densities provides an effective estimate of the joint density, which avoids some of the inherent challenges of direct joint density estimation.

## 4 Exposure Set Identification

The above presentation of the estimation of the marginal, joint and interaction shift parameters assumes that the subsets of the mixture that are important with respect to the outcome, as well as the pairs that have evidence of statistical interaction, are known a priori. However, in finite samples with a large number of mixture variables,  $\mathbf{A}$ , including all components of the mixture as potentially impactful exposures and all possible interactions will result in unacceptable sample variability (and potential nonnormality). Therefore, we

propose using a data-adaptive target parameter approach Hubbard et al. [2016] to use sample splitting to “discover” the relevant components and interactions among the mixture variables and estimate the resulting data-adaptively defined parameters.

We propose a K-fold cross-validation in which the sample data are split into K-folds of roughly equal size. For example, consider  $K = 10$ , and define  $k = 1$ . The  $K - 1/K$  portion of the sample is used to define the parameter of interest (here 90%) and the  $1/K$  (10%) is used to estimate the parameters. Let  $T_{n,k} \subset \{1, \dots, n\}$  denote the observations indices in the k-th training sample and  $V_{n,k}$  denote the observations indices in the k-th validation sample for  $k = 1, \dots, K$ . The following paragraphs describe how through cross-validation the  $T_{n,k}$  (training) portion of the data is used to identify important variable sets in the mixture and  $V_{n,k}$  (validation) is used to estimate our stochastic shift intervention parameters.

## 4.1 Identifying Interactions in the Mixture Using Training Data

The discovery of variables and interactions of mixture variables that are important for the prediction of the outcome is done using an ensemble method: the discrete Super Learner (SL) van der Laan Mark et al. [2007]. This algorithm employs a cross-validation mechanism, optimizing over a library of candidate algorithms to select the estimator with the best empirical fit. We use a discrete SL to select the best fitting estimator from a library of different sieve-based estimators that use basis splines and their tensor products, allowing the model to capture intricate nonlinear relationships as linear combinations of lower-dimensional basis functions while remaining interpretable. These include packages like `earth` Milborrow. Derived from `mda:mars` by T. Hastie and R. Tibshirani. [2011] , `polySpline` Ripley and Venables [2021], and `ha19001` Coyle et al. [2022]. In our current implementation, our candidate algorithms used in the library are all based on `earth`.

Because **earth** has many hyperparameters such as the number of interactions, how knot points are searched, etc. we include **earth** models with various parameters and select the best one based on cross-validation. This still falls within the framework of Super Learning. We employ this estimator for  $E[Y|\mathbf{A}, W]$  used in the data-adaptive discovery procedure using the training data. For example, for  $k = 1$  in a 10 fold CV, this includes all folds not equal to 1. In the context of high-dimensional mixture analysis, traditional ANOVA techniques are likely inadequate due to their limitations in handling nonlinear relationships. To address this, we introduce a non-parametric extension, Non-parametric Analysis of Variance (NP-ANOVA), following the selection of the best-fitting estimator through the Super Learner algorithm. The NP-ANOVA approach is designed to decompose the variance of the response variable by attributing it to contributions from individual basis functions utilized in the chosen model. This method is versatile and is applicable across various model structures such as MARS, HAL, among others. The central idea is to assess the relative importance of each basis function in explaining the variance of the response variable. The procedure can be summarized as follows. 1. From the model selected by the Super Learner, we extract the basis functions employed by the model, 2. Utilize these basis functions to build a GLM, allowing for a structured analysis of the contributions of bases, 3. Perform a Type 3 ANOVA on the GLM. This step involves systematically evaluating the change in explained variance when each basis function is omitted, thus assessing their individual contributions, 4. For each basis function, calculate an F-statistic, quantifying its impact on the explanatory power of the model, 5. Group and sum the F-statistics according to the variable sets corresponding to each basis, such as individual variables (e.g.,  $A_1$ ) or interactions (e.g.,  $A_3 - A_4$ ), 6. Employ quantile-based thresholding on aggregated F-statistics to discern the most influential variable sets. For example, selecting the top 25%

of variable sets or including all sets by setting the threshold at 0.

## 4.2 Estimation of Shift Interventions on Discovered Variable Sets

Treating these variable sets as fixed, we then estimate the resulting data-adaptively defined parameters using TMLE for marginal and joint stochastic shift interventions. Using the training data, the nuisance functions  $g_n$  and  $Q_n$  are trained. The TMLE update step is performed using these training estimates to estimate  $\epsilon$ . With the validation data, we obtain estimates for  $g_n$  and  $Q_n$  and apply  $\epsilon$  to debias our initial plug-in for our estimated stochastic shift target parameter using the validation data. In our running example, the validation data is data that correspond to  $k = 1$ . This procedure describes CV-TMLE Hubbard et al. [2018, 2016] which is the infrastructure we use to estimate our target parameter. Readers interested in the details of this procedure are directed to these resources.

With the estimates for our parameter complete for the validation for  $k = 1$ , we would then move on to  $k = 2$  and repeat the sections 2-4. Upon completion of the cross-estimation procedure, a pooled TMLE update provides a summary measure of the target parameter across k-folds. Specifically, we stack the predictions for each nuisance parameter from the estimation samples and run a pooled TMLE update on the cumulative initial estimates. The resulting average is then used for parameter estimation. The pooled estimate across the folds can be succinctly represented as  $\theta = \frac{1}{K} \sum_k \Psi_{F_{T_{n,k}}} (V_{n,k}) (P_0)$ . Where  $\Psi_{F_{T_{n,k}}}$  identifies optimal exposure sets and subsequently formulates a plug-in estimator using training data  $T_{n,k}$ .  $V_{n,k}$  refers to our data's estimation sample for deriving our estimates.

It is possible that the same interactions are not found in every fold. Here, our approach deviates from the standard data-adaptive target parameter method. In defining parameters normally, one would define, for example, the interaction with maximum impact defined by

some measure (like our F-statistic or another measure) or perhaps create ranks. However, this may result in many different interactions being included in the top rank, which makes interpretation difficult. In this setting, the analyst is then required to interpret only the fold-specific results, which are statistically valid but have low power, and perhaps report the proportion of folds the interaction was found. In the proposed framework, we gain power by pooling in folds with consistent estimates, but the pooled result is difficult to interpret as well because these estimates do not incorporate information from folds with null results. As such, in refining our approach to pooled TMLE estimation, our goal is to integrate both the non-null estimates from the estimation samples and the null values. To address this, we propose a weighted average approach that combines our original pooled estimate with the implied null value, which we define as 0.

Specifically, let  $n_0$  denote the number of folds where the null is implied, and let  $n_1$  represent the number of folds with non-null estimates. The variance of the "null" estimate,  $var(\Psi_{\text{null}})$ , is estimated using the variance of the original pooled estimates,  $var(\hat{\Psi}_{\text{pooled}})$ , as follows  $var(\Psi_{\text{null}}) = \left( var(\hat{\Psi}_{\text{pooled}}) \right) \cdot \frac{n_1}{n_0}$ . We then calculate the weighted average of the original pooled estimate and the null value  $\hat{\Psi}_{\text{pooled}}^* = \frac{w_1 \cdot \hat{\Psi}_{\text{pooled}} + w_0 \cdot \Psi_{\text{null}}}{w_0 + w_1}$ , where  $w_1 = \frac{1}{var(\hat{\Psi}_{\text{pooled}})}$  and  $w_0 = \frac{1}{var(\Psi_{\text{null}})}$ . The variance of this new pooled estimate is given by  $var(\hat{\Psi}_{\text{pooled}}^*) = \frac{1}{w_1 + w_0}$ . This approach ensures that our pooled TMLE estimate reflects both the explicit estimates from folds where the variable set was selected and the implicit null values from the remaining folds. Of course, in settings where there is strong "signal" and interactions are consistently found across the folds this inverse variance approach is not needed and only the standard pooled TMLE is used. Fold-specific TMLE updates are also provided, allowing researchers to gauge consistency by comparing estimates across individual folds. Each fold-specific update applies a similar logic as the pooled update but remains confined



to the respective fold, utilizing its specific  $Q_k$  and  $h_k$  parameters. Consequently, the EIF for each fold is calculated using only validation data within the fold, providing distinct variance estimates.

### 4.3 Pooled Estimates under Data-Adaptive Delta

Stochastic interventions, particularly joint stochastic shifts that involve products of conditional densities, may be vulnerable to positivity violations. Such violations can introduce bias and inflate variance in exposure effect estimation after shift, even with sophisticated estimators like TMLE. Addressing this necessitates a restrained  $\delta$ , diminishing positivity violations, and thereby reducing bias and variance. We propose treating  $\delta$  as data-adaptive. It is determined in the training sample, adhering to positivity criteria, and subsequently applied to the validation sample. Define  $H(a_\delta, w)_i$  as the density ratio for observation  $i$  after a shift  $\delta$ . To maintain ratios below a threshold  $\lambda$ , we iteratively diminish  $\delta$  by  $\epsilon$  until:  $\forall i, H(a_\delta, w) = \frac{g_{n-k}(a_{n-k} - \delta | w)}{g_{n-k}(a_{n-k} | w)} \leq \lambda$ . Here,  $\lambda$  is preset (default is 50 in our implementation). If any predicted conditional probabilities exceed this threshold under observed exposure,  $\delta$  decreases by  $\epsilon$  (defaulted to 10% in our package). This adjustment employs training data with estimators trained therein. Should  $\delta$  remain constant across folds, the pooling involves averaging the estimates of the target parameters. For a data-adaptive  $\delta$ , where  $\delta$  may be different in different folds, we simply take the mean estimate for a pooled  $\delta$  across the folds that is paired with the pooled TMLE estimate.

## 5 Simulations

In this section, we demonstrate using simulations that our approach identifies the correct exposures and interactions used to generate the outcome and correctly estimates the

counterfactual mean difference in outcome under joint shift intervention, marginal shifts, and subsequently the comparison, our interaction parameter. We construct a data-generating process (DGP) where  $Y$  is generated from a linear combination of different effects including marginal impacts and interactions. This DGP was constructed to represent the complexity of a mixed exposure in which mixture variables are correlated but only some have an impact on the outcome.

This DGP has the following characteristics,  $O = W, A, Y$ . Let  $W = (W_1, W_2, W_3)$  denote a random vector of covariates, where  $W_1$  and  $W_2$  are bivariate normal with mean vector  $\boldsymbol{\mu} = (6, 7)$  and covariance matrix  $\boldsymbol{\Sigma}_W = \begin{pmatrix} 1 & 0.4 \\ 0.4 & 1 \end{pmatrix}$  and  $W_3$  is a binary variable with Bernoulli distribution with probability 0.5. The mean values for the components of the distribution of mixture  $A$  are calculated as  $\mu_1 = e^{W_1/2}$ ,  $\mu_2 = W_2/2$ , and  $\mu_3 = 5$ . That is, exposure 3 is not associated with the covariates. A exposure vector  $A = (A_1, A_2, A_3)$  is generated from a trivariate normal distribution with a mean vector  $\boldsymbol{\mu} = (\mu_1, \mu_2, \mu_3)$  and a covariance matrix:  $\boldsymbol{\Sigma}_A = \begin{pmatrix} 1 & 0.5 & 0.8 \\ 0.5 & 1 & 0.7 \\ 0.8 & 0.7 & 1 \end{pmatrix}$ . A fourth mixture variable was created via  $A_4 \sim \mathcal{N}(4, 2)$ . The outcome  $Y$  is then generated by:  $Y = 1.3A_4 + 0.4A_4A_1 + 0.1W_1 + 0.3W_2 + \epsilon + (A_3^2\mathbf{1}_{\{W_3=1\}} + A_3\mathbf{1}_{\{W_3=0\}})$ . Where the third component of  $A$  depends on  $W_3$ ,  $A_3$  is squared if  $W_3$  is equal to 1, and is left unchanged if it is equal to 0. In generating the outcome, this variable represents effect modification or the differential impact of  $A_3$  depending on  $W_3$ . Overall, built into this outcome-generating process there is a marginal impact of  $A_4$ , a multiplicative interaction between  $A_1$  and  $A_4$  and effect modification of  $A_3$  based on  $W_3$ . There is no effect of  $A_2$  on the outcome. This DGP was generated to reflect, although more simply, a real-world exposure situation that includes both interaction, effect

modification, and no effects.

To calculate the ground-truth counterfactual mean under a shift intervention, we simply generate a very large data set from this DGP and apply various shifts to the exposures. We applied a shift of 1 unit increase to each exposure. In the first simulation, we deterministically set the variable sets to evaluate estimates of the counterfactual outcomes under these shifts. This was done with the `var_sets` parameter in **SuperNOVA** which, if is not null, bypasses the data-adaptive determination of the variable sets in the basis functions. In the second simulation we include the data-adaptive discovery of the variable sets to provide estimates for evaluating the variable relationship identification through the basis function procedure. In our case, given this DGP, we are interested in assessing the counterfactual mean differences under shifts for  $A_4$  individually,  $A_1$  individually,  $A_4$  and  $A_1$  jointly and comparing this joint shift with the individual shifts.

## 5.1 Evaluating Performance

We assessed the asymptotic convergence to the true exposure relationships used in the DGP, as well as the convergence to the true counterfactual differences for these exposures, in each simulation. To do so, we followed the following steps 1. From this sample, we generated a random sample of size  $n$  from the DGP, 2. At each iteration, we used the training sample to define the exposure(s) and create the necessary estimators for the target parameter dependent on the variable sets. We then used the validation sample to obtain the updated causal parameter estimate using TMLE. We repeated this process for all the folds, 3. At each iteration, we output the stochastic shift estimates given the pooled TMLE.

To evaluate the performance of our approach, we calculated several metrics for each iteration, including bias, variance, MSE, confidence interval (CI) coverage, and the proportion

of instances in which the true variable relationships were identified. To visually inspect if the rate of convergence was at least as fast as  $\sqrt{n}$ , we show projections of a  $\sqrt{n}$  consistent estimator starting from the initial bias. We then calculated the variance for each estimate and used it to calculate the mean squared error (MSE) as  $\text{MSE} = \text{bias}^2 + \text{variance}$ . To account for different sample sizes, we multiply the MSE estimates by  $n$ . For each estimate, we also calculated the CI coverage of the true stochastic shift parameter given the exposure determined adaptively from the data. We calculated these performance metrics at each iteration, performing 50 iterations for each sample size  $n = (250, 500, 1000, 1500, 2000, 2500, 3000, 5000)$ . We used **SuperNOVA** with 5-fold cross-validation (to speed up calculations in the simulations) and default learner stacks (see below) for each nuisance parameter and data-adaptive parameter. Additionally, the quantile threshold to filter the basis functions based on F-statistic was set to 0 to include all basis functions used in the final best-fitting model. For each sample size, we calculate the proportion of iterations in which the correct main effects and interaction effects were discovered.

To use **SuperNOVA**, we need estimators for  $\bar{Q} = E(Y|A, W)$  and  $g_n = p(A|W)$  (conditional density). **SuperNOVA** provides default algorithms to be used in a Super Learner van der Laan Mark et al. [2007] that are both fast and flexible. For our data-adaptive procedure, we include learners from the packages `earth` Milborrow. Derived from `mda:mars` by T. Hastie and R. Tibshirani. [2011], `polspline` Ripley and Venables [2021], and `hal9001` Coyle et al. [2022]. The results from each of these packages can be formed into a model matrix, on which we can fit an ANOVA to obtain the resulting linear model of basis functions. To estimate  $\bar{Q}$ , we include estimators for the Super Learner from `glm`, `elastic net` Tay et al. [2023], `random forest` Wright and Ziegler [2017], and `xgboost` Chen and Guestrin [2016]. For the semiparametric density estimator  $g_n$ , we create estimators based on homoscedastic

errors (HOSE) and heteroscedastic errors (HESE) from the same estimators used in  $\bar{Q}$ .

## 5.2 Results

**SuperNOVA consistently discovers interactions.** The interaction effect was identified in 100% of the folds in all sample sizes. This indicates that, at least in this simple simulation, the default learners are flexible enough to capture the interaction effect. **Target parameters estimated by SuperNOVA converge to truth at a  $1/\sqrt{n}$  rate,** **Figure 1 A** shows the absolute bias, CI coverage, mean squared error, and standard deviation as the sample size increases to 5000. For bias, MSE and standard deviation, there is a converge to zero at sample size 5000. For coverage, the average coverage for each target parameter was: individual shift: 98%; joint shift: 96%; interaction: 96%.

To establish SuperNOVA’s estimator validity, it is essential to demonstrate that its sampling distribution approximates a normal distribution centered at 0, with its variance decreasing as sample size grows. This is evaluated through the sampling distribution of each estimate. **Figure 1 B** illustrates the probability density of the standardized bias relative to true estimates in 50 iterations for varying sample sizes, indicating convergence to a mean 0 normal distribution as sample size increases. Specifically, **Figure 1 B. Individual Effect** displays the convergence of the standardized bias for a single variable shift towards a normal distribution with mean 0 and standard deviation 1. Likewise, **Figure 1 B. Joint Effect** and **Figure 1 B. Interaction** depict the sampling distributions for dual variable shifts and interaction parameter estimates, respectively. In all scenarios, the distributions align with a standard normal distribution as the sample size increases, ensuring the reliability of our inferential approach.

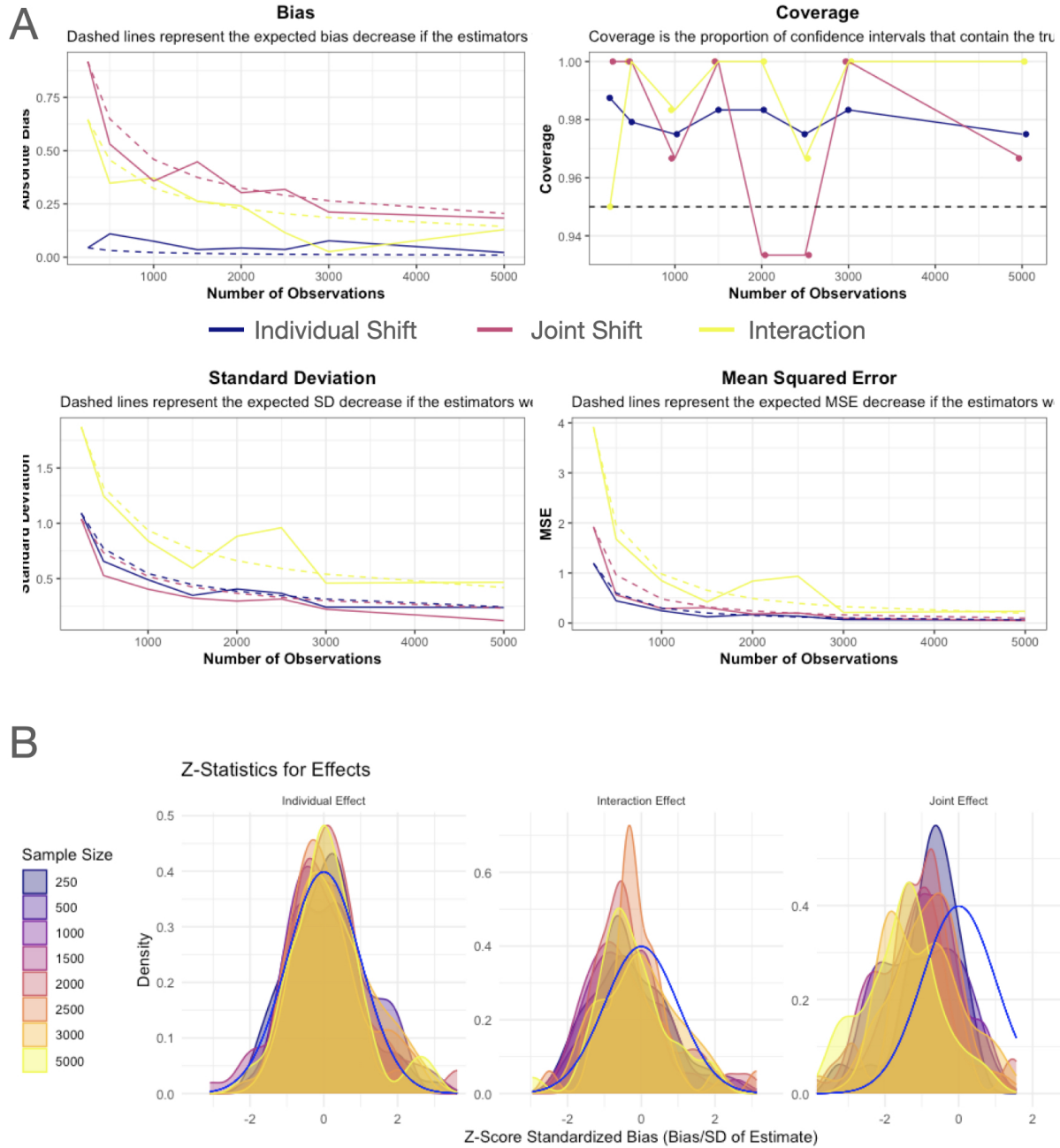


Figure 1: A. Bias, CI, Standard Deviation and MSE for Each Parameter Across Sample Sizes: These metrics represent results from CV-TMLE, that is bias is w.r.t. the data adaptive target parameter where we use CV to identify the exposure and then estimate. B. Bias Standardized by Standard Error Compared to Ground-Truth Outcome Under Shift Interventions

## 6 Applications

### 6.1 Analysis of NIEHS Synthetic Mixtures Data

The NIEHS synthetic mixtures data is a commonly used data set to evaluate the performance of statistical methods for mixtures. These synthetic data can be considered the results of a prospective cohort study, where the outcome cannot cause exposures, and correlations between exposure variables can be thought of as caused by common sources or modes of exposure. The variable  $W$  can be assumed to be a potential confounder and not a collider. The data set has 7 exposures ( $A_1 - A_7$ ) with a complex dependency structure based on endocrine disruption. Two groups of exposure ( $A_1, A_2, A_3$  and  $A_5, A_6$ ) lead to high correlations within each group.  $A_1, A_2, A_7$  positively contribute to the outcome,  $A_4, A_5$  have negative contributions, while  $A_3$  and  $A_6$  have no impact on the outcome. Rejecting  $A_3$  and  $A_6$  is difficult due to their correlations with the members of the cluster group. This correlation and effects structure is biologically plausible, as different congeners of a group of compounds may be highly correlated but have different biological effects. Exposures have various agonistic and antagonistic interactions, a breakdown of the variables sets and their relationships are:  $A_1, A_2$  both increase  $Y$  by concentration addition,  $A_1 - A_4, A_2 - A_4, A_1 - A_4, A_2 - A_4$  competitive antagonism,  $A_1 - A_7, A_2 - A_7$  supra-additive or synergistic,  $A_4, A_5$  both additively decrease  $Y$ ,  $A_4 - A_7, A_5 - A_7$  unusual antagonism. Synthetic data and the key for dataset 1 are available on GitHub. This resource shows the interactions and marginal dose relationships built into the data. Given these toxicological interactions, we expect these sets of variables to be determined in **SuperNOVA**. For example, we might expect a positive counterfactual result for  $A_1, A_2, A_7$  and negative results for  $A_4$  and  $A_5$ . Likewise, in the case for antagonistic relationships such as  $A_1-A_5$  (third row in Table 1),

we would expect a joint shift to come closer to the null, since A5 antagonizes the positive effects of A1. For A1 and A2, we would expect the joint shift to be close to the sum of individual shifts (not much interaction), but for A1 and A7 we expect to estimate more than an additive effect (some interaction). The NIEHS data set has 500 observations and 9 variables.  $W$  is a binary confounder. Of course, in this data there is no ground truth, like in the above simulations, but we can gauge **SuperNOVA**’s performance by determining if the correct variable sets are used in the interactions and if the correct variables are rejected.

We apply **SuperNOVA** to this NIEHS synthetic data using a 20-fold CV. For computational simplicity, we considered a small learner library consisting of a main terms linear regression and random forest models for estimation  $g$  and  $Q$ . For the discovery of the exposure variable sets, we built 13 earth models with various hyperparameters. We parallelize over the cross-validation to test computational run-time on a newer personal machine an analyst might be using. We use a delta of 1 for all the exposures in the mixture. We present the pooled TMLE results and the pooled TMLE results with inverse variance for null folds. Due to space limitations we do not show fold specific results but these are provided to the user.

## 6.2 NIEHS Synthetic Data Results

**SuperNOVA** accurately rejects exposures  $A_3, A_6$ , finding the correct marginal effects for  $A_1, A_2, A_4, A_5, A_7$  consistently in all folds. Specifically, A1: 100%, A2: 85%, A4: 95%, A5: 100%, A7 100%. The interactions were harder to identify consistently, and the strongest interaction between A5 and A7 was detected in 70% of the folds. Specifically, A1-A2: 10%, A1-A5: 45%, A1-A7: 20%, A2-A7: 50%, A4-A5: 15%, A4-A7: 5%, and A5-A7: 70%. Our analysis of the NIEHS Mixtures Data reveals the marginal effects of various exposures on endocrine disruption outcomes, measured as the change in outcome per unit increase



in relative exposure. Each exposure’s effect, along with its confidence interval, p-value, and the proportion of folds in which the effect was observed, are reported as follows. A1 demonstrated a significant increase in the outcome by 5.69 units, with a 95% CI of 4.81 to 6.57, identified consistently across all folds (proportion = 1.0), and a p-value  $< 0.01$ . A5 Showed a significant decrease in the outcome by -3.41 units, with a 95% CI of -4.28 to -2.54, consistently observed across all folds (proportion = 1.0), and a p-value  $< 0.01$ . A7 indicated a significant increase in the outcome by 3.40 units, with a 95% CI of 2.47 to 4.33, found in all folds (proportion = 1.0), and a p-value  $< 0.01$ . A4 had a non-significant effect of -0.36 units (inverse variance pooled), with a 95% CI of -1.69 to 0.22 and observed in 95% of folds, with p-value of 0.29. A2 exhibited a significant increase in the outcome by 1.82 units (inverse variance pooled), with 95% CIs of 0.93 to 2.72, found in 85% of folds, and both with p-values  $< 0.01$ . These findings align with the direction and relative strengths of association built into this synthetic data DGP.

We found three significant interaction effects defined as deviations when considering joint shifts in exposures compared to the sum of individual shifts. These interactions were for exposures A1-A5, A1-A7, and A2-A7, which aligns with the interactions built into this DGP. For the interaction between A1 and A5, we observe that a unit shift in A1 individually leads to an increase of 10.40 (9.08-11.73) in the outcome. On the contrary, a unit change in A5 individually shows a decrease of -2.86 (-4.10 - -1.62), suggesting an antagonistic relationship between these exposures. When both A1 and A5 are simultaneously shifted by one unit, the expected outcome under joint shift is 0.49 (-0.66 - 1.63), thus generally nullifying each exposure effect, making the interaction effect -7.26 (-8.59 - -5.92),  $p < 0.001$ . This effect was found in 45% of folds. The interaction between A1 and A7 shows that individual changes in A1 and A7 lead to increases of 14.74 (13.14 - 16.34) and 2.42 (0.62 - 4.22), respectively.

However, the joint shift in X1 and X7 only increases endocrine function by 5.31 (3.65 - 6.98), resulting in an interaction effect of -11.76 (-13.4 - -10.12). This effect indicates that the joint shift is significantly less than expected under additive assumptions. This interaction was found in 20 % folds. The shift in A2 led to a 5.56 (4.19 - 6.93) and A7 a 2.83 (1.65 - 4.02), the joint shift a 4.89 (3.75 - 6.04), which led to an interaction effect of -3.86 (-5.24 - -2.48),  $p < 0.001$ , proportion of folds = 50%. Individual shifts in A5 and A7 result in changes of -2.74 (-3.70 - -1.78) and 2.61 (1.60 - 3.62), respectively. However, the interaction effect of their joint shift is -0.02 (-1.03 - 0.98), which leads to an interaction effect of -0.05 (-1.02 - 0.93), found in 70% of the folds. This suggests that these two exposures have an additive antagonism, which is built into the DGP. Due to space limitations, we do not provide fold-specific results and more details, but these are provided on github package page. Although our detection of interactions was not found in every fold (due potentially to a low sample size), we identified the majority of interactions built into these data.

### 6.3 Comparison to Quantile G-Computation

Quantile g-computation is a favored approach in environmental epidemiology’s mixture analyses. Estimates the joint effect of increasing all exposures by one quantile, based on linear assumptions, as:  $Y_i = \beta_0 + \sum_{j=1}^d \beta_j X_{ji}^q + \beta Z_i + \epsilon_i$ . Here,  $X^q$  represents the quantized components of the mixture. The methodology consists of transforming the components of the mixture into quantiles and then adding the coefficients of the linear model to produce a summary measure of the mixture,  $\Psi$ . However, several limitations emerge: 1. Quantiles may not accurately reflect the exposure-response relationship, which can be nonmonotonic in substances like endocrine disruptors, 2. For a comprehensible mixture estimate  $\Psi$ , it presumes an additive relationship of quantiles, 3. Given the intricate

nature of mixtures, interactions are vital. Including interactions in quantile g-computation complicates the interpretation, as the exposure’s proportional contribution becomes variable depending on other factors’ levels, 3. This method lacks flexibility in covariate control. Our application to the NIEHS dataset with 4 quantiles, excluding interactions, yielded a scaled positive effect size of 6.28 (encompassing  $A_1, A_2, A_3, A_7$ ) and a negative effect size of -3.68 (involving  $A_4, A_5, A_6$ ). Discrepancies arise when compared to the NIEHS baseline, incorrectly including  $A_3, A_6$ . Incorporating interactions compounds the challenge. Our approach with all exposure interactions showed a joint impact of main effects of 0.02 (-3.16 - 3.20),  $p = 0.99$  and interaction effects of 0.59 (-0.71 - 1.90),  $p = 0.37$ . Considering the parameter count and a sample size of  $n = 500$ , it is not surprising that these estimates are not significant. However, even attempts to rigorously analyze 2-way or 3-way interactions introduce an array of complications, underscoring mixtures as an inherently data-adaptive issue and the insufficiencies of conventional methods on even straightforward synthetic datasets.

## 6.4 Methods Applied to NHANES Dataset

The National Health and Nutrition Examination Survey (NHANES) 2001-2002 cycle serves as the foundation of our analysis. This data source, known for its credibility in the public health domain, boasts interviews with 11,039 individuals. Of this subset, 4,260 provided blood samples and willingly consented to DNA analysis. The data set used aligns with that of Mitro et al. [2016] focusing on the correlation between persistent exposure to organic pollutants (POPs), specifically those binding to the aryl hydrocarbon receptor (AhR) and extended leukocyte telomere length (LTL). However, this subset was further refined to ensure complete exposure data, yielding 1007 participants for our analysis,

compared to 1003 in the initial study by Mitro et al. In alignment with protocols detailed by Mitro et al. Mitro et al. [2016], exposure was quantified, focusing on 18 congeners. These include 8 non-dioxin-like PBCs, 2 non-ortho PCBs, 1 mono-ortho PCB, 4 Dioxins, and 4 Furans. All congeners underwent lipid serum adjustments using an enzymatic summation methodology. The telomere length, was analyzed using the quantitative polymerase chain reaction (qPCR) methodology Mitro et al. [2016]. This technique measures the T/S ratio by comparing the length of the telomere to a standardized reference DNA. To enhance accuracy, samples underwent triple assays in duplicate, generating an average from six data points. The CDC conducted a blinded quality control assessment. Our modeling accounted for several covariates, including demographic factors such as age, sex, race / ethnicity and level of education, as well as health indicators such as BMI, serum cotinine, and blood cell distribution and count. Categorizations for race/ethnicity, education, and BMI are consistent with previous studies. Furthermore, this comprehensive dataset is integrated into the **SuperNOVA** package for replicable analysis.

We configured our methodology using default learners and employed a 20-fold CV without a quantile threshold for the F-statistic of the basis function. The built-in algorithms of the Super Learner were used to identify variable associations in the discovery procedure, using linear terms and two-way interactions of earth models and various hyperparameters (13 models in total). Given the data range, a  $\delta$  value of 2 was fixed for all exposures, denoting a focus on counterfactual changes in telomere length for an increase in 2 ng / g or pg / g across exposures that predict telomere length depending on the scale of exposure.

## 6.5 Comparing NHANES Furan Results to Previous Work

In our analysis of the 18 POPs, furan 2,3,4,7,8-pncdf emerged consistently across all 20 folds. None of the other chemicals were featured in any fold. The pooled TMLE estimated a 0.02 (0.03 - 0.001) decrease in telomere length after a 2 pg / g increase in furan 2,3,4,7,8-pncd which was significant at  $p = 0.04$ . Results in individual folds showed similar effects. The Mitro et al. [2016] summarize the results of the workshop. They state that clustering methods identified high, medium, and low POP exposure groups with longer log-LTL observed in the high exposure group. Principal component analysis (PCA) and exploratory factor analysis (EFA) revealed positive associations between overall POP exposure and specific POPs with log-LTL. Penalized regression methods identified three congeners (PCB 126, PCB 118, and furan 2,3,4,7,8-pncdf) as potentially toxic agents. WQS identified six POPs (furans 1,2,3,4,6,7,8-hxcdf, 2,3,4,7,8-pncdf, and 1,2,3,6,7,8-hxcdf, and PCBs 99, 126, 169) as potentially toxic agents with a positive overall effect of the POP mixture. BKMR found a positive linear association with furan 2,3,4,7,8-pncdf, suggestive evidence of linear associations with PCBs 126 and 169, a positive overall effect of the mixture, but no interactions among congeners. These results (in the supervised methods) controlled for the same covariates. Interestingly, although we corroborate the finding of furan 2,3,4,7,8-pncdf, specifically in the BKMR method (the most flexible method used), our results show a negative association. Additionally, we do not find associations of any other POP used in any fold, meaning that in the best-fitting spline model, no basis functions for any of the other POPs were used. The inverse association we find compared to these other methods could be a result of our  $Q$  model being a Super Learner, which can model relationships perhaps missed in these other methods. Through this NHANES example, we underscore the ability of **SuperNOVA** in discerning pertinent variable relationships in complex

mixture data, subsequently producing estimates. The consolidated findings allow for a clear understanding of the potential changes in outcomes in different exposure scenarios, improving the interpretability of the results. Interestingly, despite the heterogeneity of the findings of other methods, we identify only one chemical possibly related to a reduced telomere length, furan 2,3,4,7,8-pncdf, which warrants further investigation.

## 7 Discussion

In our study, we developed a semiparametric statistical model to estimate interaction effects in mixed exposures, focusing on identifying and quantifying exposure sets that influence outcomes. Using data-adaptive target parameters and using targeted maximum likelihood estimation (TMLE) within a cross-validation framework, we achieved asymptotically unbiased estimates of interaction effects. Our approach offers several advantages, including robustness to the number of exposures and the complexity of the data-generating process, and it provides interpretable results that improve understanding of drug synergies and environmental health impacts. Unlike traditional interaction analysis methods, our model minimizes assumptions, yielding more reliable and interpretable estimates of interaction effects and focuses on causal quantities. Our methodology faces two primary limitations. First, the computational intensity of the density estimation step, though mitigated by parallel processing, remains a challenge. Alternatives such as recasting density estimation as a classification problem could offer efficiency improvements, but would require iterative refitting of the classifier. Second, the identification of exposure sets varies between cross-validation folds, introducing variability that demands careful and consistent reporting to ensure reproducibility and reliability of results. Future enhancements, including the incorporation of algorithms like glmnet and the highly adaptive lasso (HAL), are expected to

stabilize identification processes. It is crucial for findings to be reported only if they demonstrate consistency across multiple cross-validation folds, with transparent communication about the variability of these findings.

In future research, we aim to address the limitations and expand the capabilities of our approach. Key directions include improving density estimation. We plan to explore the transformation of density estimation into a classification problem using Bayesian probability. This shift promises to improve computational efficiency and incorporate a wider range of machine learning algorithms. Refining pooling strategies and testing is also required; we will develop and evaluate new pooling strategies, such as kernel estimators to estimate the sampling distribution of our estimates with null effects and sampling from null distributions to refine pooled estimates incorporating the null, hopefully improving the robustness of our inverse variance strategy. We can also focus beyond two-way interactions to include higher-order complexities. We also intend to investigate alternative TMLE strategies that may offer better performance, especially in smaller samples. This includes direct computation of influence functions for interaction parameters and novel estimation techniques for clever covariates. To facilitate adoption, we have developed the **SuperNOVA** R package, available on GitHub, offering researchers software to apply our proposed methodology for the analysis of mixtures, this package has been peer reviewed by the Journal of Open-Source Software McCoy et al. [2023].

## References

Jennifer F. Bobb, Linda Valeri, Birgit Claus Henn, David C. Christiani, Robert O. Wright, Maitreyi Mazumdar, John J. Godleski, and Brent A. Coull. Bayesian kernel machine regression for estimating the health effects of multi-pollutant mixtures. *Biostatistics*, 16

(3):493–508, 2014. ISSN 14684357. doi:10.1093/biostatistics/kxu058.

Tianqi Chen and Carlos Guestrin. XGBoost: A scalable tree boosting system. In *Proceedings of the 22nd ACM SIGKDD International Conference on Knowledge Discovery and Data Mining*, KDD '16, pages 785–794, New York, NY, USA, 2016. ACM. ISBN 978-1-4503-4232-2. doi:10.1145/2939672.2939785. URL <http://doi.acm.org/10.1145/2939672.2939785>.

Wei-Chia Chen, Ammar Tareen, and Justin B Kinney. Density estimation on small data sets. *Phys. Rev. Lett.*, 121(16):160605, October 2018.

Jeremy R Coyle, Nima S Hejazi, Rachael V Phillips, Lars WP van der Laan, and Mark J van der Laan. *hal9001: The scalable highly adaptive lasso*, 2022. URL <https://github.com/tlverse/hal9001>. R package version 0.4.3.

Miguel García-Villarino, Antonio J. Signes-Pastor, Margaret R. Karagas, Isolina Riaño-Galán, Cristina Rodríguez-Dehli, Joan O. Grimalt, Eva Junqué, Ana Fernández-Somoano, and Adonina Tardón. Exposure to metal mixture and growth indicators at 4–5 years. A study in the INMA-Asturias cohort. *Environmental Research*, 204, 2022. ISSN 10960953. doi:10.1016/j.envres.2021.112375.

Alan Hubbard, Chris Kennedy, and Mark Laan. *Data-Adaptive Target Parameters*, pages 125–142. 01 2018. ISBN 978-3-319-65303-7. doi:10.1007/978-3-319-65304-4\_9.

Alan E. Hubbard, Sara Kherad-Pajouh, and Mark J. Van Der Laan. Statistical Inference for Data Adaptive Target Parameters. *International Journal of Biostatistics*, 12(1):3–19, 2016. ISSN 15574679. doi:10.1515/ijb-2015-0013.

Iván Díaz Muñoz and Mark van der Laan\*. Population Intervention Causal Effects



- Based on Stochastic Interventions. *Biometrics.*, 68(2):541–549, 2012. ISSN 15378276. doi:10.1111/j.1541-0420.2011.01685.x.Population. URL <https://www.ncbi.nlm.nih.gov/pmc/articles/PMC3624763/pdf/nihms412728.pdf>.
- Alexander P. Keil, Jessie P. Buckley, Katie M. O’Brien, Kelly K. Ferguson, Shanshan Zhao, and Alexandra J. White. A quantile-based g-computation approach to addressing the effects of exposure mixtures. *arXiv*, 128(April):1–10, 2019. ISSN 23318422. doi:10.1097/01.ee9.0000606120.58494.9d.
- Benjamin Lengerich, Sarah Tan, Chun Hao Chang, Giles Hooker, and Rich Caruana. Purifying Interaction Effects with the Functional ANOVA: An Efficient Algorithm for Recovering Identifiable Additive Models. *Proceedings of Machine Learning Research*, 108: 2402–2412, 2020. ISSN 26403498.
- David McCoy, Alejandro Schuler, Alan Hubbard, and Mark van der Laan. Supernova: Semi-parametric identification and estimation of interaction and effect modification in mixed exposures using stochastic interventions in r. *Journal of Open Source Software*, 8(91): 5422, 2023. doi:10.21105/joss.05422. URL <https://doi.org/10.21105/joss.05422>.
- Archana J. McEligot, Valerie Poynor, Rishabh Sharma, and Anand Panangadan. Logistic lasso regression for dietary intakes and breast cancer. *Nutrients*, 12(9):1–14, 2020. ISSN 20726643. doi:10.3390/nu12092652.
- S. Milborrow. Derived from mda:mars by T. Hastie and R. Tibshirani. *earth: Multivariate Adaptive Regression Splines*, 2011. URL <http://CRAN.R-project.org/package=earth>. R package.
- Susanna D Mitro, Linda S Birnbaum, Belinda L Needham, and Ami R Zota. Cross-sectional associations between exposure to persistent organic pollutants and leukocyte telomere

- length among us adults in nhanes, 2001–2002. *Environmental health perspectives*, 124(5): 651–658, 2016.
- Naveen N. Narisetty, Bhramar Mukherjee, Yi-Hau Chen, Richard Gonzalez, and John D. Meeker. Selection of nonlinear interactions by a forward stepwise algorithm: Application to identifying environmental chemical mixtures affecting health outcomes. *Statistical Medicine*, 38(9):1582–1600, Apr 2019. doi:10.1002/sim.8059.
- B. D. Ripley and W. Venables. *polspline: Polynomial Spline Routines*, 2021. URL <https://CRAN.R-project.org/package=polspline>. R package version 1.1.26.
- Steven Roberts and Michael A. Martin. Using supervised principal components analysis to assess multiple pollutant effects. *Environmental Health Perspectives*, 114(12):1877–1882, 2006. ISSN 00916765. doi:10.1289/ehp.9226.
- Kenneth J Rothman, Sander Greenland, and Alexander M Walker. Concepts of interaction. *Am J Epidemiol*, 112(4):467–470, 1980.
- Donald B Rubin. Estimating causal effects of treatments in randomized and nonrandomized studies. *J. Educ. Psychol.*, 66(5):688–701, October 1974.
- Donald B Rubin. Causal inference using potential outcomes. *J. Am. Stat. Assoc.*, 100(469): 322–331, March 2005.
- J. Kenneth Tay, Balasubramanian Narasimhan, and Trevor Hastie. Elastic net regularization paths for all generalized linear models. *Journal of Statistical Software*, 106(1):1–31, 2023. doi:10.18637/jss.v106.i01.
- Mark J van der Laan. Statistical inference for variable importance. *Int. J. Biostat.*, 2(1), February 2006.

- J. van der Laan Mark, Polley Eric C, and Hubbard Alan E. Super learner. *Statistical Applications in Genetics and Molecular Biology*, 6(1):1–23, 2007. URL <https://EconPapers.repec.org/RePEc:bpj:sagmbi:v:6:y:2007:i:1:n:25>.
- Tyler J VanderWeele. On the distinction between interaction and effect modification. *Epidemiology*, 20(6):863–871, 2009.
- Tyler J VanderWeele and Mirjam J Knol. A tutorial on interaction. *Epidemiologic Methods*, 3(1):33–72, 2014.
- Tyler J VanderWeele and James M Robins. Directed acyclic graphs, sufficient causes, and the properties of conditioning on a common effect. *Am J Epidemiol*, 166(10):1096–1104, 2007.
- Marvin N. Wright and Andreas Ziegler. ranger: A fast implementation of random forests for high dimensional data in C++ and R. *Journal of Statistical Software*, 77(1):1–17, 2017. doi:10.18637/jss.v077.i01.
- Wenjing Zheng and MJ van der Laan. Asymptotic theory for cross-validated targeted maximum likelihood estimation. *U.C. Berkeley Division of Biostatistics Working Paper Series*, (273), 2010. URL <http://biostats.bepress.com/ucbbiostat/paper273/>.